On using Perfectly Matched Layer for the Euler equations with a non-uniform mean flow

Fang Q. Hu*

Department of Mathematics and Statistics

Old Dominion University, Norfolk, Virginia 23529

A Perfectly Matched Layer (PML) for linearized Euler equaitons with a non-uniform mean flow is presented. The PML is formulated following a proper space-time transformation so that in the transformed coordinates all dispersive waves have consistent phase and group velocity. It is shown that the parameter for the proper space-time transformation has to be determined through a study of the dispersion relations of linear waves supported by a non-uniform mean flow. PML equations for both bounded and unbounded flows are given. Furthermore, the stability of the proposed PML equations is also considered. Numerical examples that demonstrate the validity and effectiveness of PML as an absorbing boundary condition are presented.

Introduction

Non-reflecting boundary condition is necessary in any computation involving wave propagation to an open physical domain. It remains a significant challenge particularly for fluids related problems having non-linear or non-constant coefficient governing equations. The need for accurate non-reflecting boundary conditions has become even greater after the substantial progress in recent years in the discretization methods, such as the utilization of high-order schemes and unstructured meshes as well as orders-of-magnitude improvement in high performance computing power. Non-reflecting boundaries are often the sources of most significant numerical errors in practical computations.

In this paper, we develop non-reflecting boundary conditions for the linearized Euler equations with a non-uniform mean flow based on the Perfectly Matched Layer (PML) methodology. PML was originally designed as an absorbing boundary condition for computational electro-magnetics.^{6,9,11,26,31,33} The significance of the PML technique lies in the fact that, for multi-dimensional problems, the absorbing zone so constructed can be theoretically reflectionless for electro-magnetic waves of any angle and frequency. However, early works on the extension of the PML technique to the Euler equations in fluid dynamics indicated that a direct adaptation of the original split formulation could lead to numerical instability problems.^{1,16,17,27}

Substantial progresses have been made in recent studies regarding the PML for fluids dynamics.^{3,5,13,18,27} It has now been recognized that the cause for instability in previous PML formulations

is that the Euler equations, with a convective mean flow, support waves that have opposite signs in their phase and group velocities and these waves are actually amplified and become unstable waves under the original PML formulation.¹⁸ Consequently, a necessary condition for a wave to be absorbed, and not amplified, in the PML zone is that the phase and group velocities of all dispersive waves must be consistent. The stability of PML is thus intimately linked to the underlying physical waves and their phase and group velocities. Recognizing this, new formulations of PML have been proposed recently.^{3, 12, 13, 18} For instance, in [18], a stable PML for the linearized Euler equations with a uniform mean flow was proposed. It employed a proper space-time transformation before applying the PML technique so that in the transformed coordinates all waves have consistent phase and group velocities. This has led to a dynamically stable and highly accurate absorbing boundary condition for the linearized Euler equations with a uniform mean flow. The method used in [18] has also been recently applied to the shallow water equation in geophysics.²

The focus of this paper is on the formulation of stable PML for Euler equations with parallel non-uniform mean flows. Recently, in [13], a formulation of PML for linearized Euler equation with a uniform mean flow was extended to non-uniform flows, in which one parameter of the layer was adjusted numerically to maintain stability. The main issue, as we will show in this paper, is how to choose a priori the proper space-time transformation when the mean flow is non-uniform so that all waves supported by the governing equations have consistent phase and group velocities in the transformed coordinates. In this paper, we will show that the proper space-time transformation can be determined based on the

^{*}Professor, Senior Member AIAA

Copyright © 2004 by F. Q. Hu. Published by the American Institute of Aeronautics and Astronautics, Inc. with permission.

study of dispersive waves of the Euler equations, so that in the transformed coordinates all waves have the same sign for the phase and group velocities. After the application of such a space-time transformation, stable PML equations will be constructed following the technique used in [18].

The rest of the paper is organized as follows. In the next section, recent progresses are reviewed and the importance of understanding the dispersion relations of linear waves on the construction of stable PML is discussed. Then, a detailed study on all dispersive waves supported by the Euler equations with a wall bounded non-uniform mean flow is presented. Following a proper space-time transformation, derivation of PML equation is given, followed by a study on the stability of the proposed PML equation. Finally, numerical examples are presented that demonstrate the validity and efficiency of the PML as an absorbing boundary condition.

Dispersive waves and the stability of PML

In this section, we give a brief review of recent works on PML for the Euler equations (see, e.g., [1,3,5,12,13,18,27]). It shall become obvious the importance of understanding the dispersive waves of the physical system in the construction of stable PMLs.

One view of the PML technique is that it is a complex change of variables in the frequency domain $^{7,\,9,\,11,\,26,\,31}$ and this view will be assumed in our investigation. For simplicity, all discussions in this section will be limited to the construction of a vertical x-layer which involves a PML complex change of variable for x as

$$x \longrightarrow x + \frac{i}{\omega} \int_{x_0}^x \sigma_x dx \tag{1}$$

where $\sigma_x > 0$ is the absorption coefficient (a function of x) and x_0 is the location of the PML/Euler interface. Other alternative forms of (1) are possible, such as the one given in [4] for long time stability, but they will not alter the basic arguments provided below. As a heuristic argument, consider a wave ansatz of the form

$$e^{i(kx-\omega t)}$$
. (2)

Under the complex change of variable (1), it becomes

$$e^{i(kx-\omega t)}e^{-\frac{k}{\omega}\int_{x_0}^x \sigma_x dx}.$$
 (3)

The second factor in expression (3) indicates that the wave amplitude decays exponentially in the PML zone if and only if the condition

$$\frac{k}{\omega} \int_{x'}^{x} \sigma_x dx > 0 \tag{4}$$

is satisfied as the wave propagates from any arbitrary location x' in the PML zone. This means that the PML is only absorbing for a wave that propagates to the right $(x \ increasing)$ with $k/\omega>0$ or propagates to the left $(x \ decreasing)$ with $k/\omega<0$. In other words, for the amplitude of the wave to be reducing (and not increasing) in the PML domain, the direction of wave propagation should be consistent with the sign of k/ω or, equivalently, the phase velocity ω/k .^{5, 18} Since the direction of propagation of a dispersive wave is determined by the group velocity, this necessary condition has been expressed nicely in [5] as

$$\frac{\omega}{k} \frac{d\omega}{dk} > 0. \tag{5}$$

That is, for the PML technique to yield stable absorbing boundary conditions, the phase and group velocities of the physical waves must be consistent and have the same sign. Conversely, any wave of the original physical system having opposite signs in its phase and group velocities will be amplified and result in instability in the PML domain. Condition (5) links intimately the construction of stable PMLs to the dispersion relation $(\omega = \omega(k))$ of the physical waves under investigation.

This necessary condition for stable PML was recognized in several recent studies.^{5, 13, 18, 27} For instance, in [18], it was pointed out that, in the presence of a convective mean flow, the Euler equations support acoustic waves that have a positive group velocity but a negative phase velocity and these waves were actually amplified in previous PML formulations. It was further proposed in [18] that a proper space-time transformation be applied to the Euler equations before applying the PML technique so that under the transformed coordinates all linear waves supported by the Euler equations have consistent phase and group velocities. For the linearized Euler equation with a uniform mean flow in the xdirection, the proper space-time transform involved a transformation in time of the form

$$\bar{t} = t + \beta x,\tag{6}$$

where

$$\beta = \frac{\bar{U}_0}{1 - \bar{U}_0^2} \tag{7}$$

in which \bar{U}_0 is the *uniform* mean flow Mach number.¹⁸ It follows that the corresponding transformation in the frequency-wavenumber space is

$$\bar{k} = k + \beta \omega, \bar{\omega} = \omega.$$
 (8)

The value of β in (7) was determined so that the dispersion relation of the convective acoustic waves, namely.

$$(\omega - \bar{U}_0 k)^2 - k^2 - k_y^2 = 0$$

becomes the following in the transformed space

$$\bar{\omega}^2/(1-\bar{U}_0^2)-(1-\bar{U}_0^2)\bar{k}^2-k_y^2=0$$

for which the phase and group velocities are consistent. 18 This transformation is the same as the "Prandtl-Glauert" transformation in aerodynamics. In [18], a new PML equation was formulated by applying the complex change of variable (1) in the transformed coordinates. The new PML formulation was dynamically stable and perfectly matched to the Euler equation for the acoustic, vorticity and entropy waves. The importance of the space-time transformation (6) and the particular choice for β in (7) were also confirmed in recent independent formulations in [3,12,13]. For example, in [13], the importance of the transformation (6) was reflected by forming a special wave ansatz. An extension of PML to non-uniform mean flows was also given in [13] where an equivalent value for β , called μ , was adjusted by numerical experiments that gave stable solutions.

The question becomes whether it is possible to determine a priori the proper space-time transformation for the Euler equations with an arbitrary non-uniform mean flows so that, in the transformed coordinates, all linear waves have consistent phase and group velocities. We will show in the next section that, for a parallel non-uniform mean flow, it is possible to find the value for β in (6), actually a unique choice, based on a study of the dispersion relations of the physical waves.

Linear waves of Euler equations with a non-uniform mean flow bounded by solid walls

Let the linearized Euler equations with a parallel non-uniform mean flow be written as

$$\frac{\partial \mathbf{u}}{\partial t} + \mathbf{A} \frac{\partial \mathbf{u}}{\partial x} + \mathbf{B} \frac{\partial \mathbf{u}}{\partial y} + \mathbf{C} \mathbf{u} = 0$$
 (9)

in which

$$\mathbf{u} = \begin{pmatrix} \rho \\ u \\ v \\ p \end{pmatrix}, \ \mathbf{A} = \begin{pmatrix} \bar{U} & \bar{\rho} & 0 & 0 \\ 0 & \bar{U} & 0 & \frac{1}{\bar{\rho}} \\ 0 & 0 & \bar{U} & 0 \\ 0 & 1 & 0 & \bar{U} \end{pmatrix},$$

$$\mathbf{B} = \begin{pmatrix} 0 & 0 & \bar{\rho} & 0 \\ 0 & 0 & 0 & 0 \\ 0 & 0 & 0 & \frac{1}{\bar{\rho}} \\ 0 & 0 & 1 & 0 \end{pmatrix}, \text{ and } \mathbf{C} = \begin{pmatrix} 0 & 0 & \frac{d\bar{\rho}}{dy} & 0 \\ 0 & 0 & \frac{d\bar{U}}{dy} & 0 \\ 0 & 0 & 0 & 0 \\ 0 & 0 & 0 & 0 \end{pmatrix}$$

where u and v are velocity components in the x and y directions respectively, non-dimensionalized by a

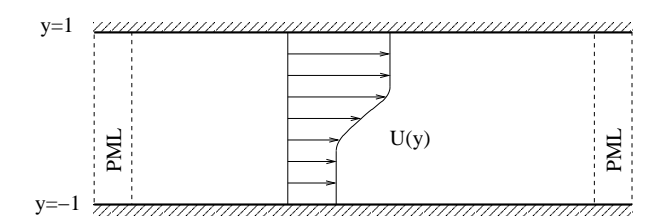


Figure 1 A schematic of a bounded parallel non-uniform mean flow.

reference speed of sound a_o ; ρ is the density, non-dimensionalized by a reference value ρ_o ; and p is the pressure, non-dimensionalized by $\rho_o a_o^2$. Also, the space variables x and y are non-dimensionalized by a reference scale ℓ_o and time t is non-dimensionalized by ℓ_o/a_o . The mean velocity $\bar{U}(y)$ and density $\bar{\rho}(y)$ are functions of y only and the mean pressure is constant.

As the discussion in the previous section shows, the construction of stable PML is intimately connected to the dispersion relations of the linear waves supported by the Euler equations. In this section, we conduct a study of physical waves of (9) in a parallel flow bounded by solid walls at $y=\pm 1$, as shown in Figure 1. For this purpose, a linear wave analysis for (9) will be carried out numerically. In this approach, we seek wave solutions of the form

$$\mathbf{u}(x, y, t) = \hat{\mathbf{u}}(y)e^{i(kx - \omega t)} \tag{10}$$

where ω and k are the frequency and wave-number respectively. By substituting (10) into the Euler equation (9), we get an eigenvalue problem

$$-i\omega\hat{\mathbf{u}} + ik\mathbf{A}\hat{\mathbf{u}} + \mathbf{B}\frac{d\hat{\mathbf{u}}}{dy} + \mathbf{C}\hat{\mathbf{u}} = 0$$
 (11)

with these homogeneous boundary conditions,

$$\frac{d\hat{u}}{dy} = \hat{v} = \frac{d\hat{p}}{dy} = \frac{d\hat{\rho}}{dy} = 0 \text{ at } y = \pm 1.$$
 (12)

This eigenvalue problem will be solved by a spectral collocation method which is a standard method in hydrodynamic stability analysis. 10,22,25 Further details are given in the Appendix. It yields a complete spectrum of all normal modes supported by (11). The eigenvalue ω of (11) as a function of given wave number k defines the dispersion relation $\omega = \omega(k)$.

As a specific example, we will demonstrate the dispersion relations of linear waves associated with a shear flow of mean velocity

$$\bar{U}(y) = \frac{1}{2} [(U_1 + U_2) + (U_1 - U_2) \tanh(\frac{2y}{\delta})]$$
 (13)

and mean density

$$\bar{\rho}(y) = \frac{1}{\bar{T}(y)} \tag{14}$$

with

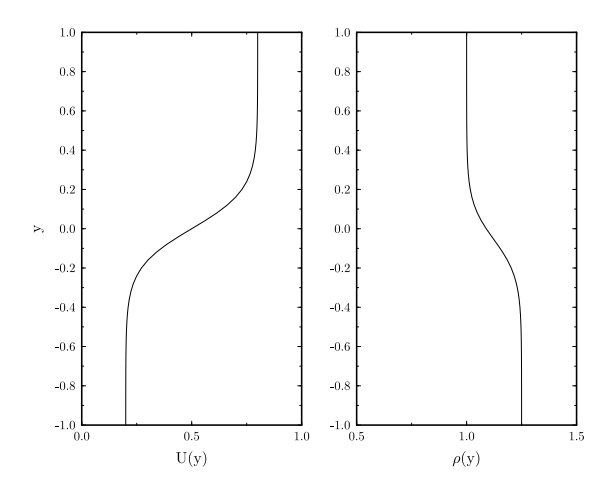


Figure 2 Mean velocity and density used in the example.

$$\bar{T}(y) = T_1 \frac{\bar{U} - U_2}{U_1 - U_2} + T_2 \frac{U_1 - \bar{U}}{U_1 - U_2} + \frac{\gamma - 1}{2} (U_1 - \bar{U})(\bar{U} - U_2)$$

where the mean temperature $\bar{T}(y)$ is determined by the Crocco relation for compressible flows. $\gamma=1.4$. The mean flow parameters chosen for the example are as follows:

$$U_1 = 0.8$$
, $U_2 = 0.2$, $\delta = 0.4$, $T_1 = 1$, $T_2 = 0.8$.

The mean velocity and density profiles are plotted in Figure 2. Both are non-constant.

Figure 3 shows the dispersion relation diagram of all the normal modes of (11), i.e., real part of ω v.s. k. The imaginary part is zero for all wave modes except the Kelvin-Helmholtz instability wave which will be shown later.

In this dispersion diagram, we see two families of waves. One family has phase speed between $U_{min}=0.2$ and $U_{max}=0.8$, shown between dashed lines in the ω_r-k diagram. These are "vortical" modes that convect with the mean flow. We see that for the vortical modes, both the group and phase velocities are positive. Therefore condition (5) is satisfied. We note that one of the vortical modes is the Kelvin-Helmholtz instability wave supported by the present mean flow profile. An enlarged graph is shown in Figure 4 for the real and imaginary parts of ω as functions of k where the Kelvin-Helmholtz wave is highlighted by circles.

The other family of waves in the dispersion diagram Figure 3 are "acoustic" modes. A closer examination of the acoustic modes indicates that they always have a phase speed supersonic relative to part of the mean flow. Furthermore, they are dispersive waves, 32 where $\omega/k \neq constant$. Figure 3 also shows that the acoustic modes do not always have consistent phase and group velocities. A triangle on

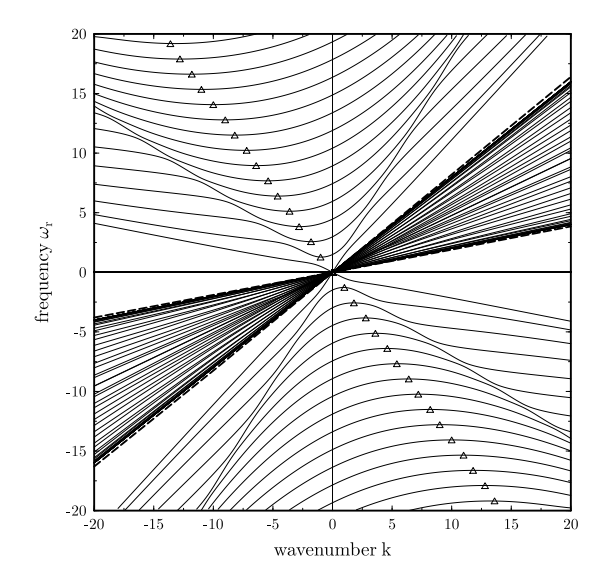


Figure 3 Dispersion relation diagram. Triangles denote the points of zero group velocity. Dashed lines are $\omega_r = U_1 k$ and $\omega_r = U_2 k$.

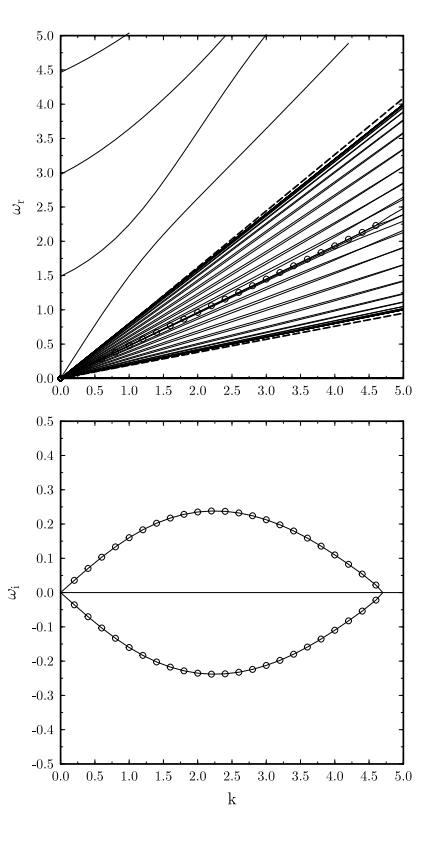


Figure 4 Dispersion relation diagram enlarged from Figure 3. Top: real part of ω v.s. k; bottom: imaginary part of ω v.s. k. The circles highlight the Kelvin-Helmholtz instability wave.

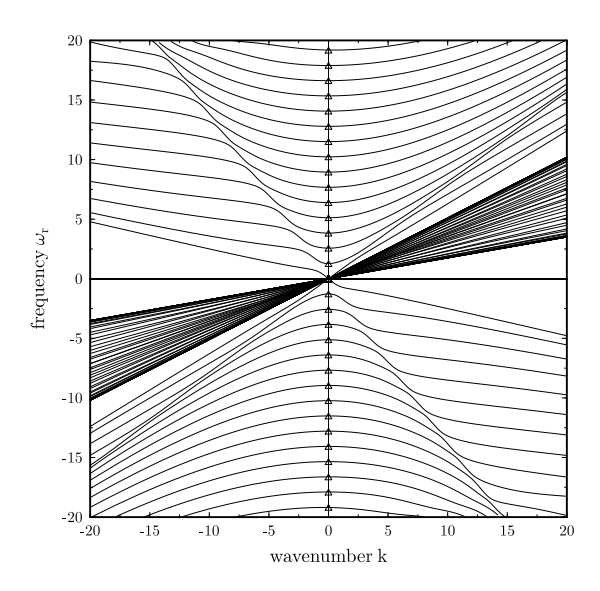


Figure 5 Dispersion relation diagram in transformed coordinates. Triangles denote the points of zero group velocity.

the acoustic modes indicates the location where the group velocity is zero, i.e., $d\omega_r/dk=0$. As we can see, for the acoustic modes in the upper left and lower right quarters in Figure 3 that lie between the triangle and the vertical axis, their phase velocity (ω_r/k) is negative but their group velocity $(d\omega_r/dk)$ is positive. By the argument provided in the previous section, applying directly the PML complex change of variable (1) to the Euler equation (9) without a proper space-time coordinate transformation will result in these waves being amplified and becoming unstable modes.

To find the proper space-time transformation, we note that, remarkably, the locations of zero group velocity points on the dispersion diagram (Triangles in Figure 3) appear to lie on a straight line. This implies that space-time transformation (6), which incurs a change in the frequency-wave number space of the form (8), can again be used to "correct" the dispersion relation. The obvious choice for β in (6) and (8) is

$$\beta = -\frac{1}{c_0} \tag{15}$$

where c_0 is the slope of the line of triangles ($\omega_r = c_0 k$) in Figure 3. This also suggests that the proper value for β is uniquely defined for a particular given mean flow profile. For the current example, examination of the eigenvalues for the dispersion relation indicates $c_0 \approx -1.407$.

The dispersion relation diagram in the transformed coordinates is shown in Figure 5. Now all the waves have consistent phase and group velocities and satisfy condition (5).

It is important to point out that it is not accidental that all points of zero group velocity fall in a line. For other types of subsonic mean flow profiles, including mixing layers, jets, wakes, it was found, at least numerically, that the points of zero group velocity on the dispersion diagram for the acoustic modes were always closely lined. Two further examples of jet and plane Poiseuille flows are shown in Figure 6. It is also worth pointing out that if part of the mean flow is supersonic, it has been found that each acoustic mode will have two locations where the group velocity becomes zero, 20 which would make the transformation (6) ineffective.

Derivation of PML equations

Unsplit formulation

Once the value of β for the proper space-time transformation (6) has been determined based on the dispersion relations of the acoustic modes, the derivation of PML for the Euler equations will be carried out as follows. We shall first apply the space-time transformation (6) to the governing equations so that all dispersive waves have consistent phase and group velocities. Then, the PML complex change of variable is applied in the transformed coordinates. And finally the PML equation in the original physical time domain is obtained. Details are given below.

Under transformation (6), we have these changes in the partial derivatives,

$$\frac{\partial}{\partial t} \to \frac{\partial}{\partial \overline{t}}, \quad \frac{\partial}{\partial x} \to \frac{\partial}{\partial x} + \beta \frac{\partial}{\partial \overline{t}}$$
 (16)

and the Euler equation (9) in transformed coordinates becomes

$$(\mathbf{I} + \beta \mathbf{A}) \frac{\partial \mathbf{u}}{\partial \bar{t}} + \mathbf{A} \frac{\partial \mathbf{u}}{\partial x} + \mathbf{B} \frac{\partial \mathbf{u}}{\partial y} + \mathbf{C} \mathbf{u} = 0.$$
 (17)

The PML technique will now be applied to the transformed equation (17). We first write the equation in the frequency domain,

$$-i\bar{\omega}(\mathbf{I} + \beta \mathbf{A})\tilde{\mathbf{u}} + \mathbf{A}\frac{\partial \tilde{\mathbf{u}}}{\partial x} + \mathbf{B}\frac{\partial \tilde{\mathbf{u}}}{\partial y} + \mathbf{C}\tilde{\mathbf{u}} = 0, \quad (18)$$

in which $\mathbf{u}(x, y, \bar{t}) = \tilde{\mathbf{u}}(x, y)e^{-i\bar{\omega}\bar{t}}$ is assumed.

To construct the PML equation for the vertical x-layer, we apply the PML complex change of variable (1) to the frequency domain equation (18) which involves a change in the partial derivative for x as

$$\frac{\partial}{\partial x} \longrightarrow \frac{1}{1 + \frac{i\sigma_x}{2}} \frac{\partial}{\partial x} \tag{19}$$

where σ_x is a positive function of x. That is, equation (18) is modified to be

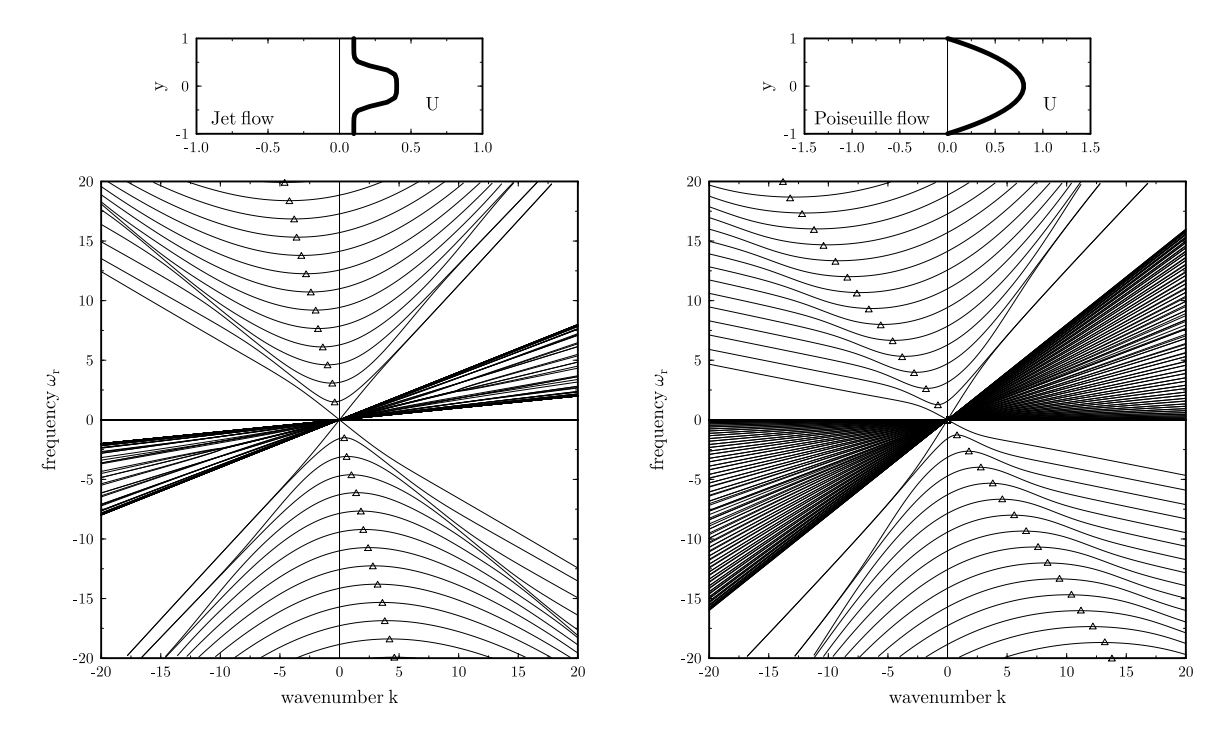


Figure 6 Dispersion relation diagram of a jet (left) and a channel Poiseuille flow (right). Triangles denote the points of zero group velocity.

$$-i\bar{\omega}(\mathbf{I} + \beta \mathbf{A})\tilde{\mathbf{u}} + \frac{1}{1 + \frac{i\sigma_x}{\bar{\omega}}} \mathbf{A} \frac{\partial \tilde{\mathbf{u}}}{\partial x} + \mathbf{B} \frac{\partial \tilde{\mathbf{u}}}{\partial y} + \mathbf{C}\tilde{\mathbf{u}} = 0.$$
(20)

Equation (20) is the PML equation for the x-layer in the frequency domain. It will now be written back in the time domain by following an unsplit approach used in [7,11,18,31]. By multiplying the equation with $(1 + \frac{i\sigma_x}{\Omega})$, we get

$$(-i\bar{\omega} + \sigma_x)(\mathbf{I} + \beta \mathbf{A})\hat{\mathbf{u}} + \mathbf{A}\frac{\partial \hat{\mathbf{u}}}{\partial x} + (1 + \frac{i\sigma_x}{\bar{\omega}})\mathbf{B}\frac{\partial \hat{\mathbf{u}}}{\partial y} + (1 + \frac{i\sigma_x}{\bar{\omega}})\mathbf{C}\hat{\mathbf{u}} = 0.$$

The equivalent time domain equation for the above is easily found to be

$$(\mathbf{I} + \beta \mathbf{A})(\frac{\partial \mathbf{u}}{\partial \bar{t}} + \sigma_x \mathbf{u}) + \mathbf{A} \frac{\partial \mathbf{u}}{\partial x} + \mathbf{B}(\frac{\partial \mathbf{u}}{\partial y} + \sigma_x \frac{\partial \mathbf{q}}{\partial y}) + \mathbf{C}(\mathbf{u} + \sigma_x \mathbf{q}) = 0$$
(21)

where q is an auxiliary variable defined as

$$\frac{\partial \mathbf{q}}{\partial t} = \mathbf{u}.\tag{22}$$

Finally, when (21) is written in the original physical variables (x, y, t), we get the following PML equation for (9) with non-uniform mean flows,

$$\frac{\partial \mathbf{u}}{\partial t} + \mathbf{A} \frac{\partial \mathbf{u}}{\partial x} + \mathbf{B} \left(\frac{\partial \mathbf{u}}{\partial y} + \sigma_x \frac{\partial \mathbf{q}}{\partial y} \right) + \mathbf{C} (\mathbf{u} + \sigma_x \mathbf{q}) + \sigma_x \mathbf{u} + \sigma_x \beta \mathbf{A} \mathbf{u} = 0$$
(23)

where the equation for \mathbf{q} is that given in (22). It is only necessary to introduce \mathbf{q} inside the PML domains.¹⁸

Absorption of hydrodynamic instability waves

It is well known that linearized Euler equations can support hydrodynamic instability waves, for example, the Kelvin-Helmholtz instability for jets and mixing layers where the mean velocity flow profile has an inflection point. The PML should be absorbing to all waves including the instability and evanescent waves. There are generally two kinds of hydrodynamic instabilities, namely the absolute and convective instabilities.²³ For numerical simulations, we are mostly concerned with the convective instability waves that grow spatially and propagate with the mean flow to the outflow boundary. A simple argument on the phase and group velocities, given below, will show that the PML formulated here will always absorb convective instability waves.

Suppose that the mean flow is from left to right. Then the group velocity of a convective instability wave is positive, i.e., $\frac{d\omega_r}{dk} > 0.$

Furthermore, by an extension of the semi-circle theorem (in the theory of hydrodynamic stability) to compressible flows, it was shown in [8] that the phase speed of any instability wave is bounded by the mean velocity, i.e.,

$$0 < U_{min} \le \frac{\omega_r}{k} \le U_{max}. \tag{24}$$

Therefore, the phase and group velocities of a convective instability wave have the same sign and condition (5) is always satisfied, as the other vortical

modes discussed in the previous section. This means that the spatial growth rate of convective instability waves will always be reduced in the PML zone. To completely annihilate the instability waves, the PML absorption rate should be designed such that it is greater than the spatial growth rate of the instability waves.

Value for β

The parameter β in equation (23) is a critical number for ensuring the stability of the PML equation. In the previous section, the value for β has been determined as the negative reciprocal of the phase velocity c_0 of acoustic wave modes whose group velocities are zero. In other words, if in general $D(\omega, k) = 0$ is the dispersion relation, then

$$c_0 = \frac{\omega_0}{k_0} \text{ and } \beta = -\frac{1}{c_0}$$
 (25)

where $\omega_{\scriptscriptstyle 0}$ and $k_{\scriptscriptstyle 0}$ are the roots to the coupled equations

$$\begin{cases} D(\omega_{\scriptscriptstyle 0},k_{\scriptscriptstyle 0})=0 \\ \frac{\partial D}{\partial k}(\omega_{\scriptscriptstyle 0},k_{\scriptscriptstyle 0})=0 \end{cases}$$
 (26)

Although for certain shear flows, acoustic modes have been found and studied extensively in the past, for example for jets, 28 shear layers, $^{14, 15, 29}$ wakes 34 and boundary layers, 24 an explicit and direct relationship between the phase speed $c_{\rm o}$ define in (25) and an arbitrary mean flow profile has not been available. The spectral collocation method, details given in the Appendix, provides a general way of determining the dispersion relation for arbitrary mean flows. A special case is worth mentioning, however. If the mean density is constant, i.e., $\bar{\rho}(y)=1$, it has been found that a reasonably good prediction of β for practical purposes is

$$\beta = \frac{\bar{U}_m}{1 - \bar{U}_m^2} \tag{27}$$

where \bar{U}_m is the average mean velocity for a domain in $y \in [a, b]$ as

$$\bar{U}_m = \frac{1}{b-a} \int_a^b \bar{U}(y) dy. \tag{28}$$

Stability of the PML equations

When the value of β in the PML equation (23) is determined based on the dispersion relations of linear waves as described earlier, all the physical waves of the Euler equations become absorbed in the PML domain, and their amplitudes are reduced exponentially as the waves travel in the PML domain. However, with the introduction of the axillary variable \mathbf{q} , the order of partial differential equations has increased (doubled). As a result of this, the PML equations (23) and (22) can admit additional nonphysical waves. It is important that these additional

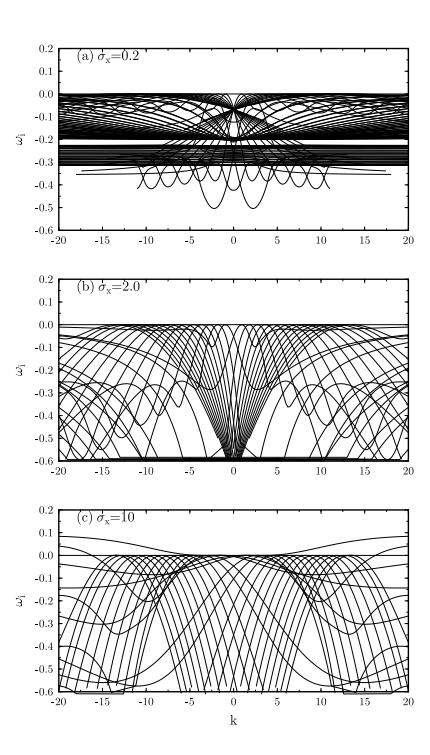


Figure 7 Imaginary part of all wave modes. (a) $\sigma_x = 0.2$, (b) $\sigma_x = 2.0$, (c) $\sigma_x = 10.0$.

wave modes are not exponentially growing. In this section, we study this issue and carry out a stability analysis for the PML equations (23) and (22).

Following the similar approach used for the analysis of the Euler equation (9), we seek solutions to (23) and (22) of the form

$$\mathbf{u}(x, y, t) = \hat{\mathbf{u}}(y)e^{i(kx - \omega t)},\tag{29}$$

$$\mathbf{q}(x, y, t) = \hat{\mathbf{q}}(y)e^{i(kx - \omega t)}.$$
 (30)

By substituting the above into (23) and (22), we get

$$(-i\omega)\hat{\mathbf{u}} + ik\mathbf{A}\hat{\mathbf{u}} + \mathbf{B}(\frac{d\hat{\mathbf{u}}}{dy} + \sigma_x \frac{d\hat{\mathbf{q}}}{dy}) + \mathbf{C}(\hat{\mathbf{u}} + \sigma_x \hat{\mathbf{q}}) + \sigma_x \hat{\mathbf{u}} + \sigma_x \beta \mathbf{A}\hat{\mathbf{u}} = 0,$$
(31)

$$(-i\omega)\hat{\mathbf{q}} = \hat{\mathbf{u}}.\tag{32}$$

With homogeneous boundary condition (12) for $\hat{\mathbf{u}}$ and similarly for $\hat{\mathbf{q}}$, (31) and (32) again form an eigenvalue problem and can be solved by the spectral collocation method (see Appendix). For any given value k, an eigenvalue ω with a positive imaginary part would indicate an exponentially growing wave.

In Figures 7 (a), (b) and (c), we plot the imaginary part of all wave modes of (31)-(32) where the value of σ_x is taken to be a fixed constant 0.2, 2.0 and 10.0, respectively, for wave number k in the range of -20 to 20. The mean flow profile is the same as that used for the example in Figure 3. For cases (a) and (b), we see that all wave modes have the imaginary part below zero, including the original Kelvin-Helmholtz wave, indicating that the PML

equation is dynamically stable, at least for range of k considered. For case (c) where $\sigma_x = 10$, however, there are some wave modes that have emerged with positive imaginary parts and thus become unstable at high wave numbers. These modes are originated from the non-physical waves. This indicates that the PML equations (22)-(23) could have exponentially growing solutions if the value of σ_x is taken to be too large. This has been found to be typical that (22)-(23) are stable when the value of the absorption coefficient is below certain limit, let it be denoted by σ_s , but admit unstable wave modes when σ_x is greater than that limiting value σ_s . Experiments show that the limiting value varies widely depending on the particular mean flow profile. For the current example, the limiting value $\sigma_s = 3$. For other mean flow profiles, such as a linear shear mean velocity,²⁰ the limiting value has been found to be as large as 100.

In cases where the value for σ_s is too small, the fact that the PML equations (22)-(23) is stable only when $\sigma_x \leq \sigma_s$ could mean that a relatively large PML domain may be needed to achieve a desirable degree of wave absorption, because the effectiveness of a PML domain depends on the magnitude of the absorption coefficient and its total width. ^{16,19} For such cases, one practical remedy could be to use grid stretching in the PML domain, so that its effective width is increased without employing more grid points. 19, 26, 33 A grid stretching is equivalent to simply modifying the x derivative terms of the PML equation as

$$\frac{\partial}{\partial x} \to \frac{1}{\alpha(x)} \frac{\partial}{\partial x}$$
 (33)

where
$$\alpha(x) \ge 1$$
 is a smooth function. For example,
$$\alpha(x) = 1 + A \left| \frac{x - x_0}{D} \right|^s$$
 (34)

where x_0 is the start of the PML domain and D its width. Grid stretching also has a side effect of introducing numerical damping which would also improve the stability of PML even when σ_x is greater than the stability limiting value σ_s . This has been found to be quite effective in computations.

A second remedy is to modify the PML equations so that the stability limiting value σ_s can be significantly increased. One such modification is to introduce a small advection term to the equation for \mathbf{q} in (22) to get

$$\frac{\partial \mathbf{q}}{\partial t} + \epsilon \frac{\partial \mathbf{q}}{\partial x} + \sigma_x \beta \epsilon \mathbf{q} = \mathbf{u}$$
 (35)

where ϵ is to be kept small. In Figure 8, we repeat the stability calculation of 7(c) where the equation for \mathbf{q} in (22) is replaced by (35). As we can see, even with a small value of $\epsilon = 0.01$, equation (35) has a dramatic effect on reducing the growth rate of the unstable modes.

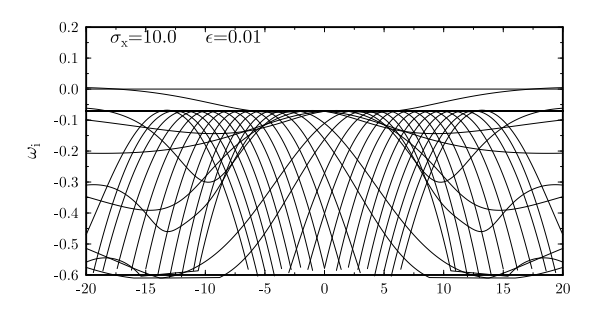


Figure 8 Imaginary part of all wave modes, where equation (22) is replaced by (35). $\sigma_x =$ 10.0, $\epsilon = 0.01$.

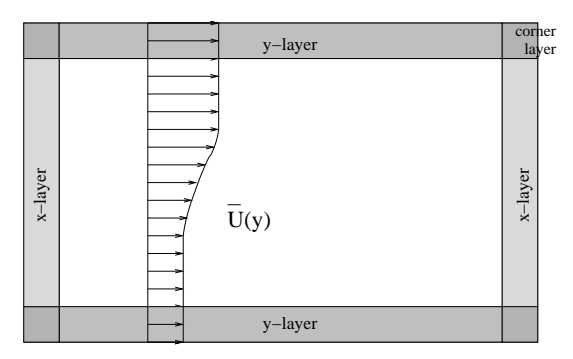


Figure 9 A schematic of an unbounded parallel non-uniform mean flow, showing x-layers, y-layers and corner layers.

PML for unbounded flows

When the flow is unbounded, PML for the horizontal y-layers are needed to terminate the computational domain at the top and bottom boundaries, as shown in Figure 9. For a parallel mean flow aligned with the x-axis, the PML equation for the y-layers can be developed by a complex change of variable in y, similar to (1) for x. Further details are referred to [18]. Here, we present a PML equation that is formally valid for all the vertical x-layers, horizontal y-layers as well as the corner layers. This is given below,

$$\frac{\partial \mathbf{u}}{\partial t} + \mathbf{A} \frac{\partial}{\partial x} (\mathbf{u} + \sigma_y \mathbf{q}) + \mathbf{B} \frac{\partial}{\partial y} (\mathbf{u} + \sigma_x \mathbf{q}) + \mathbf{C} (\mathbf{u} + \sigma_x \mathbf{q})$$

$$+(\sigma_x + \sigma_y)\mathbf{u} + \sigma_x\sigma_y\mathbf{q} + \sigma_x\beta\mathbf{A}(\mathbf{u} + \sigma_y\mathbf{q}) = 0 \qquad (36)$$

where σ_x and σ_y are the absorption coefficients and positive functions of x and y respectively. Equation (36) is perfectly matched to the Euler equation (9). In the derivation of (36), it has been assumed that the mean flow is uniform within each y-layer at the top and bottom boundaries. Except the term involving the C matrix, equation (36) is otherwise identical to the PML equation for a uniform mean flow given in [18]. Further implementation issues are referred to [18].

Equation (36) can be rewritten in a more compact form that resembles the Euler equation as follows

$$\frac{\partial \mathbf{u}}{\partial t} + \mathbf{A} \frac{\partial \mathbf{u}^y}{\partial x} + \mathbf{B} \frac{\partial \mathbf{u}^x}{\partial y} + \mathbf{C} \mathbf{u}^y + \mathbf{u}^* + \sigma_x \beta \mathbf{A} \mathbf{u}^y = 0 \quad (37)$$

where

$$\mathbf{u}^y = \mathbf{u} + \sigma_y \mathbf{q}, \ \mathbf{u}^x = \mathbf{u} + \sigma_x \mathbf{q},$$

$$\mathbf{u}^* = (\sigma_x + \sigma_y)\mathbf{u} + \sigma_x\sigma_y\mathbf{q}.$$

We note that even though the flow is physically unbounded, it becomes bounded artificially due to the truncation of the computational domain in y. Therefore, the value of β in (36) for unbounded flows should be determined in the same way as that for the bounded flows described in previous sections.

Numerical Examples

Two numerical examples will be presented where the mean flow is bounded in the first example and unbounded in the second one. Another example can be found in [20].

Wall bounded shear flow

Consider a mixing layer, with the mean velocity and density specified by (13) and (14) and bounded by solid walls at $y=\pm 1$, as shown in Figure 1. The Euler equation (9) with the following source term added to the equation of pressure,

$$s(x, y, t) = \sin(1.5t)e^{-(\ln 2)(x^2 + y^2)/0.05^2},$$
 (38)

is solved by a finite difference scheme. The computational domain is $[-1.4, 7.4] \times [-1, 1]$ with a uniform grid spacing $\Delta x = \Delta y = 0.04$. Two PML domains, each consisting of 10 grid points, are used at the inflow and outflow boundaries. The absorption coefficient σ_x inside the PML domain varies with x as

$$\sigma_x = \sigma_{max} \left| \frac{x - x_0}{D} \right|^2 \tag{39}$$

where $\sigma_{max} = 2/\Delta x = 50$. For the calculations reported here, a grid stretching of the form given in (34) is also used with the parameters being A=2 and s=2. All spatial derivatives are discretized by a 7-point DRP 4th-order central difference scheme³⁰ with a 10th-order filtering applied throughout the computational domain.¹⁷ Time integration is carried out by the optimized 5 and 6 stages Low Dissipation and Low Dispersion Runge-Kutta scheme (LDDRK56).²⁰

The added source term (38) generates acoustic waves that are reflected repeatedly by the solid walls. At the same time, it excites the Kelvin-Helmholtz instability wave of the mixing layer that propagates downstream. Figures 10 (a) and (b) show the pressure and u-velocity contours, respectively, at time

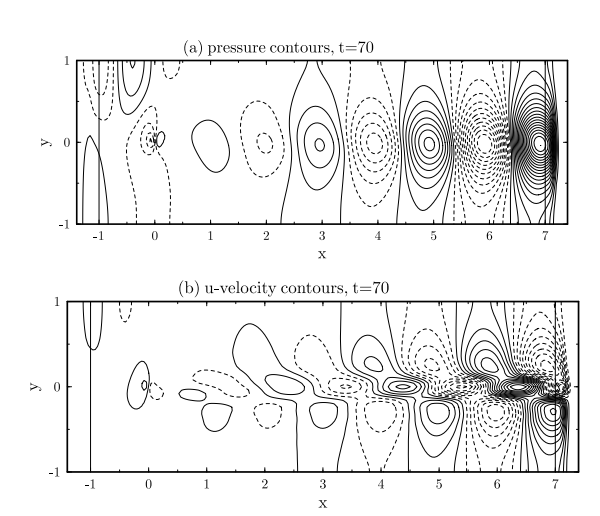


Figure 10 Contours of the numerical solution at t = 70. (a) pressure, (b) u-velocity.

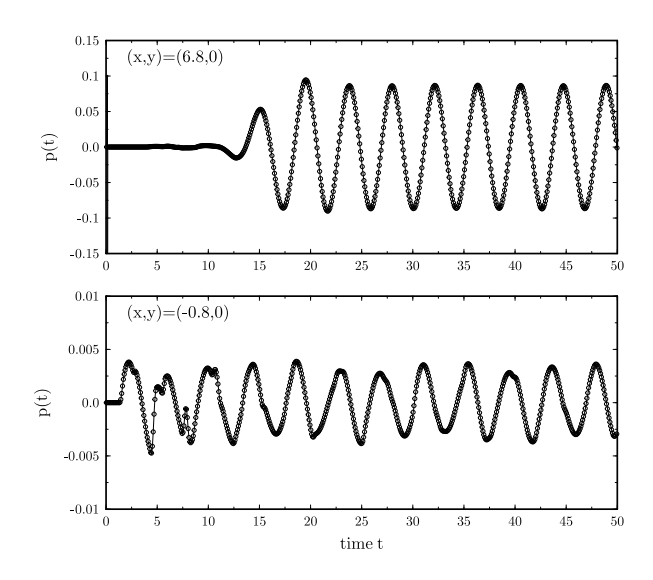


Figure 11 Pressure time history. Solid line: numerical solution; circles: reference solution.

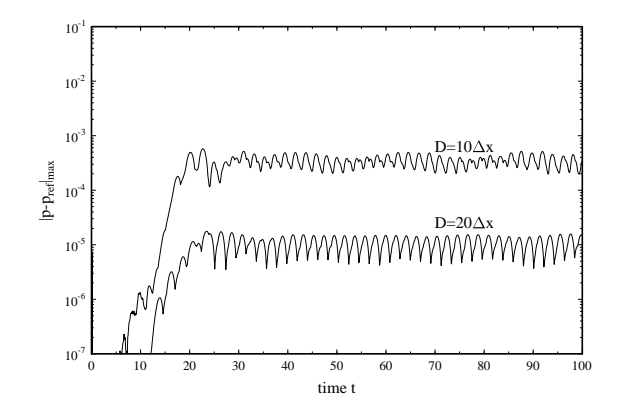


Figure 12 Maximum difference between the numerical and reference solutions along x=6.8 as a function of time.

t = 70. Clearly, wave absorption at the PML domains is quite effective.

In Figure 11, pressure as a function of time is plotted for two points located at (6.8,0) and (-0.8,0)near the outflow and inflow boundaries. The solid line is the numerical solution and circles represent a reference solution obtained by using a larger computational domain so that it is not affected by any boundary effects. Excellent agreement is found between the numerical and reference solutions with no discernible difference on the graphic scale. To quantitatively assess the effectiveness of the PML as a non-reflecting boundary condition, the maximum difference between the numerical and reference solutions on all grid points along x = 6.8 near the exit boundary is plotted in Figure 12. Judging by the fact that the amplitude of the Kelvin-Helmholtz wave at the exit is about 0.1, Figure 12 shows that the reflection error is less than 1% when 10 grid points are used in the PML domain and the reflection is less than 0.1% with 20 grid points.

We note that even though the maximum value of the absorption coefficient σ_{max} used in this example is greater than the stability limiting value σ_s for the current mean flow, no numerical instability has been observed in the computation. This suggests that grid stretching combined with numerical filtering may be sufficient to suppress the growing modes identified in Figure 7(c) beyond the stability limiting value σ_s .

Unbounded flow

In the second example, the propagation of an acoustic pulse in an unbounded shear flow, specified by (13) and (14), is simulated. The computational domain is $[-2.4, 2.4] \times [-2.4, 2.4]$ with PML domains, consisting 10 grid points, on all four sides. Equation (36) is used for all PML zones with the value of $\beta = -1/c_0$ where $c_0 = -1.416$ obtained by assuming that the flow is bounded at $y = \pm 2.4$, which is only slightly different from that in the previous example. The initial condition is

$$u = v = \rho = 0, p = e^{-(\ln 2)(x^2 + y^2)/0.2^2}$$

Figure 13 shows the u-velocity contours at t=1.5, 2.5, 3.5 and 6. The initial acoustic pulse as well as the vorticity wave induced by the shear flow are effectively absorbed at the boundaries. Figure 14 shows the time history of the u-velocity at point (1.8,0) near the outflow boundary. The numerical (solid line) and reference (circles) solutions are again in excellent agreement. The maximum difference between the numerical and reference solutions in pressure along x=1.8 is plotted in Figure 15, which shows that the use of PML causes very little reflection.

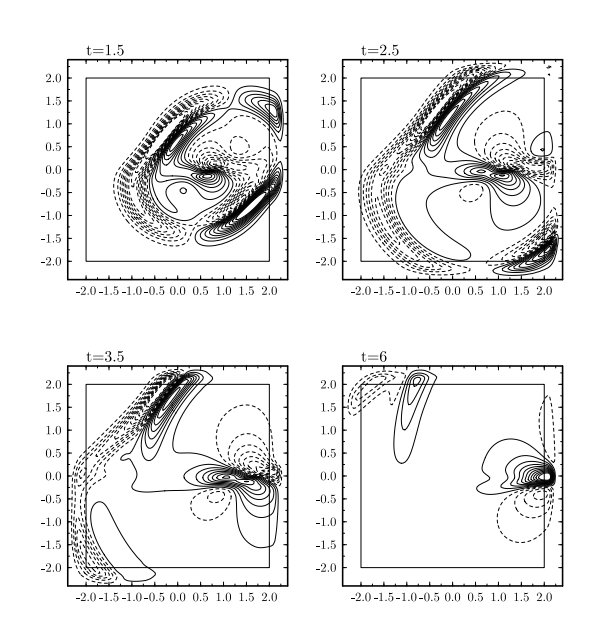


Figure 13 u-velocity contours, time as indicated.

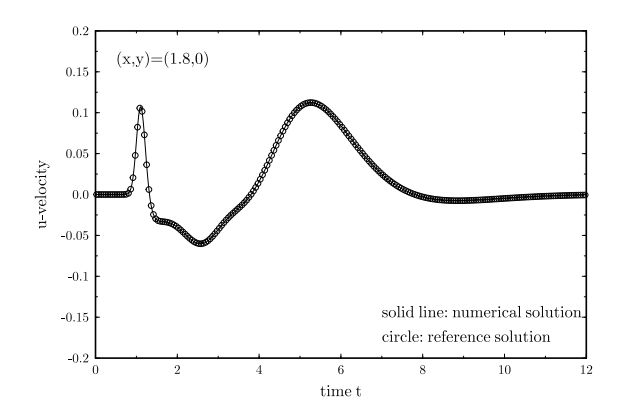


Figure 14 u-velocity time history at point (x, y) = (1.8, 0). Solid line: numerical solution; circles: reference solution.

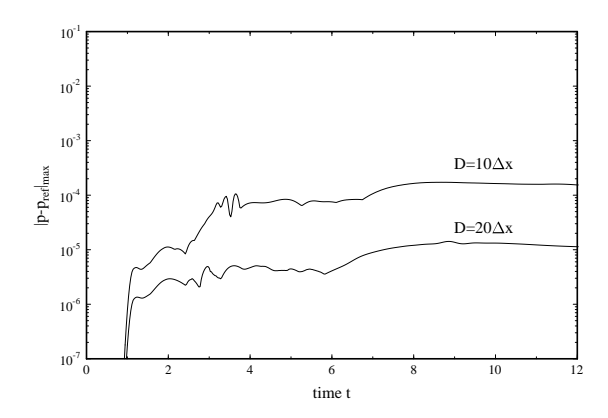


Figure 15 Maximum difference between the numerical and reference solutions along x = 1.8 as a function of time.

Conclusions

A Perfectly Matched Layer as an absorbing boundary condition for the linearized Euler equations with a parallel non-uniform mean flow is presented. It applies to both bounded and unbounded flows. It is shown that for the stability of PML it is of critical importance to apply a proper space-time transformation in the derivation of PML equation. parameter for the proper space-time transformation can be determined a priori based on the dispersion relations of acoustic modes supported by the mean flow. It is further shown that the proposed PML equation is dynamically stable for a limited range of the absorption coefficient. Numerical examples show that the PML formulated here works well for a compressible mixing layer.

Acknowledgement This work is supported in part by a grant from NASA Langley Research Center NAG1-03037.

Appendix

In this Appendix, we describe the spectral collocation method used to solve the eigenvalue problem posed by (11)-(12). Expand the solution $\hat{\mathbf{u}}(y)$ in basis polynomials as follows

$$\hat{\mathbf{u}}(y) = \sum_{n=0}^{N} \begin{pmatrix} \rho_n \phi_n(y) \\ u_n \phi_n(y) \\ v_n \psi_n(y) \\ p_n \phi_n(y) \end{pmatrix}$$
(40)

where $\{\phi_n\}$ and $\{\psi_n\}$ are formed by the Chebychev

where
$$\{\phi_n\}$$
 and $\{\psi_n\}$ are formed by the Cheb
polynomials $T_n(y)$ as
$$\psi_n(y) = \begin{cases} T_0(y) - T_{n+1}(y) & n \text{ even} \\ T_1(y) - T_{n+2}(y) & n \text{ odd} \end{cases}$$
$$\phi_n(y) = \begin{cases} \frac{1}{2} T_2(y) - T_{n+2}(y) & n \text{ even} \\ (n+2)^2 T_1(y) - T_{n+2}(y) & n \text{ odd} \end{cases}$$
The appearance (40) supports the formation (40) supports the first supports (40) supports the formation (40) supports $(40$

The expansion (40) automatically satisfies the boundary condition for $\hat{\mathbf{u}}(y)$.²² By substituting (40) into (11) and requiring that the equation be satisfied at collocation points

$$y_j = \cos(\frac{2j+1}{2N+2}\pi), \ j = 0, 1, 2, ..., N$$

we get,

$$\sum_{n=0}^{N} \left[-i\omega \begin{pmatrix} \rho_{n}\phi_{n} \\ u_{n}\phi_{n} \\ v_{n}\psi_{n} \\ p_{n}\phi_{n} \end{pmatrix} + ik\mathbf{A} \begin{pmatrix} \rho_{n}\phi_{n} \\ u_{n}\phi_{n} \\ v_{n}\psi_{n} \\ p_{n}\phi_{n} \end{pmatrix} + \mathbf{B} \begin{pmatrix} \rho_{n}\phi'_{n} \\ u_{n}\phi'_{n} \\ v_{n}\psi'_{n} \\ p_{n}\phi'_{n} \end{pmatrix} + \mathbf{C} \begin{pmatrix} \rho_{n}\phi_{n} \\ u_{n}\phi_{n} \\ v_{n}\psi_{n} \\ p_{n}\phi_{n} \end{pmatrix} \right]_{y=y_{i}} = 0$$

for j = 0, 1, 2, ..., N. This can be cast into a generalized algebraic eigenvalue problem for ω of the form $\mathbb{Q}\vec{\mathbf{u}} = \omega \mathbb{R}\vec{\mathbf{u}}$ where $\vec{\mathbf{u}}$ is a vector consisting of all the expansion coefficients in (40) and \mathbb{Q} and \mathbb{R} are $(4N+4) \times (4N+4)$ matrices.

References

- ¹S. Abarbanel, D. Gottlieb and J. S. Hesthaven, Journal of Computational Physics, Vol. 154, 266-283, 1999.
- ²S. Abarbanel, D. Stanescu and M. Y. Hussaini, Computational Geosciences, Vol. 7 (4), 265-294, 2003.
- ³E. Becache, A.-S. Bonnet-Ben Dhia and G. Legendre, SIAM J. Num. Anal., Vol. 42 (1), 409-433, 2004.
- ⁴E. Becache, P. G. Petropoulos and S. D. Gedney, INRIA Report, No. 4538, 2002.
- ⁵E. Becache, S. Fauqueux and P. Joly, Journal of Computational Physics, Vol. 188, 399-433, 2003.
- ⁶J. P. Berenger, Journal of Computational Physics, Vol. 114, 185-200, 1994.
- ⁷W. C. Chew, W. H. Weedon, IEEE Microwave Opt. Technol. Lett., Vol. 7, 599-604, 1994.
- ⁸G. Chimonas, Journal of Fluid Mechanics, Vol. 43, 833-836, 1970.
- $^9\mathrm{F.}$ Collino and P. Monk, $SIAM~J.~Sci,~Comp,~\mathrm{Vol.}~19,~\mathrm{No.}$ 6. P. 2016, 1998.
- ¹⁰P. G. Drazin and W. H. Reid, Hydrodynamic stability, Cambridge University Press, 1981.
- ¹¹S. D. Gedney, *IEEE Trans. Antennas Propagation*, Vol. 44, P. 1630, 1996.
- ¹²T. Hagstrom and I. Nazarov, AIAA paper 2002-2606, 2002.
- ¹³T. Hagstrom and I. Nazarov, AIAA paper 2003-3298, 2003.
- ¹⁴F. Q. Hu, *Physics of Fluids A*, Vol. 5, No. 6, 1420-1426,
- ¹⁵F. Q. Hu, Journal of Sound and Vibration, Vol. 183, 841-856 1995
- ¹⁶F. Q. Hu, Journal of Computational Physics, 129, 201-219, 1996.
- ¹⁷F. Q. Hu, AIAA paper 96-1664, 1996
- $^{18}\mathrm{F.~Q.~Hu},\,Journal~of~Computational~Physics,\,Vol.\,173,\,455-$ 480 2001
- ¹⁹F. Q. Hu, Absorbing boundary conditions (a review), to appear in International Journal of Computational Fluid Dynamics, 2004.
- ²⁰F. Q. Hu, Solution of aeroacoustic benchmark problems by discontinuous Galerkin method and Perfectly Matched Layer for nonuniform mean flows, to appear in the proceeding of the 4th CAA workshop on Benchmark problems, NASA CP,
- $^{21}\mathrm{F.}$ Q. Hu, M. Y. Hussaini and J. L. Manthey, Journal of Computational Physics, Vol. 124, 177-191, 1996.
- ²²F. Q. Hu and C. K. W. Tam, Physics of Fluids A, Vol. 6, No. 3, 1645-1656, 1991.
- ²³H. Huerre and P. A. Monkewitz, Annu. Rev. Fluid Mech., Vol. 22, 473, 1990.
- ²⁴L. M. Mack, Theoretical and Computational Fluid Dynamics, Vol. 2, 97-123, 1990.
- ²⁵S. A. Orszag, Journal of Fluid Dynamics, Vol. 50, 689-703, 1971.
- ²⁶P. G. Petropoulos, SIAM J. App. Math., Vol. 60, 1037-
- ²⁷C. K. W. Tam, L. Auriault and F. Cambulli, Journal of Computational Physics, **144**, 213-234, 1998.
- ²⁸C. K. W. Tam and F. Q. Hu, Journal of Fluid Mechanics, Vol. 201, 447-483, 1989.
- ²⁹C. K. W. Tam and F. Q. Hu, Journal of Fluid Mechanics, Vol. 203, 51-76, 1989.
- ³⁰C. K. W. Tam and J. C. Webb, Vol. 107, 262-281, 1993.
- ³¹E. Turkel and A. Yefet, Applied Numerical Mathematics, Vol. 27, 533-557, 1998.
- ³²G. B. Witham, Linear and nonlinear waves, Willey, 1978.
- ³³L. Zhao and A. C. Cangellaris, *IEEE Trans. Microwave* Theory Tech., Vol. 44, 2555-2563, 1996.
- ³⁴M. Zhuang, *Physics of Fluids*, Vol. 7, 2489-2495, 1995.